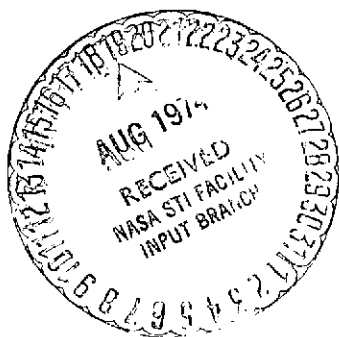Observations of Low-Energy Electrons

Upstream of the Earth's Bow Shock

by

David L. Reasoner

Department of Space Physics and Astronomy

Rice University

Houston, Texas

August, 1974

Abstract

Observations of electron fluxes with a lunar-based electron spectrometer when the moon was upstream of the earth have shown that a subset of observed fluxes are strongly controlled by the interplanetary magnetic field direction. The fluxes occur only when the IMF lines connect back to the earth's bow shock. Observed densities and temperatures were in the ranges $2-4 \times 10^{-3}$ cm^{-3} and $1.7-2.8 \times 10^{6}$ °K. It is shown that these electrons can account for increases in effective solar wind electron temperatures on bow-shock connected field lines which have been observed previously by other investigators. It is further shown that if a model of the bow shock with an electrostatic potential barrier is assumed, the potential can be estimated to be 500 volts.

A. INTRODUCTION

Observations of charged particles upstream in the solar wind whose origin was apparently at the bow shock have been reported by several authors. See, for example, Anderson [1969], Lin et al. [1974], and references therein. The common feature of these observations is that there is an interplanetary charged particle component which is strongly controlled by the direction of the interplanetary magnetic field (IMF). The particles were only observed at a particular upstream location when the field line through the observation point intersected the assumed bow shock envelope. In this paper are presented observations of low energy (40-1000 eV) electrons from a lunar-based instrument during lunar night periods. The instrument was viewing into the downstream solar wind cavity and the moon was upstream of the bow shock. Sporadic low energy fluxes were observed throughout lunar night periods, and it is shown that a subset of these electron flux events occur only when there is field line connection to the bow shock.

B. DATA

The particle measurements were made with the Charged Particle Lunar Environment Experiment (CPLEE), a component of the Apollo 14 ALSEP system. (For an instrument description see Burke and Reasoner

[1972].) Magnetic field data from the Explorer 35/Ames Research Center Magnetometer in lunar orbit provided field line geometry information.

Data from four contiguous lunar night periods in February-May 1971 were examined for the presence of electron fluxes which exhibited control by the interplanetary magnetic field direction, in particular for electron fluxes which were present only when the IMF line passing through the moon intersected the earth's bow shock. The bow shock surface was represented by an abberated hyperboloid of revolution, a model first proposed by Scudder et al. [1973]. For a given value of θ, the IMF latitude, the equation for the limiting values of the IMF longitude ϕ resulted in a quartic in cot ϕ. This equation in turn was solved for the limiting values of ϕ such that the IMF was tangent to the bow shock surface.

Because of gaps in the IMF data, it was not possible to categorize all lunar night electron flux events according to the criterion of whether or not the IMF intersected the bow shock. However, by restricting analysis to only those events where concurrent IMF data were available, it was possible to identify from the data set a total of 10 electron flux events with durations of 30 minutes or more where the electron flux exhibited strong control by the IMF direction, appearing only when the IMF line connected from the moon downstream to the bow shock. For the sake of brevity, we will refer to these events as "bow shock events" in the remainder of the paper.

An example of a bow shock event is shown in Figure 1. In this figure we display 3-minute averages of the counting rate due to 300 eV electrons (lower panel), the IMF longitude ϕ (middle panel) and the IMF latitude θ (upper panel). The limiting values of ϕ which, recall, are a function of θ are shown as dotted lines near $\pm 20°$ On this day, May 25, 1971, the solar ecliptic longitude of the moon varied from 4° to 16°, i.e. the moon was almost directly upstream from the bow shock. Two prominent, isolated events are seen, one from 0210 to 0230 and the other from 0305 to 0410. Lower intensity, shorter duration events appear near 0515 and 0620. In all these events are seen the sharp onsets and decays as the value of the IMF longitude ϕ passes through the limiting values, a feature quite typical of the total set of these bow shock events.

There are other, lower intensity electron events seen in the figure, but many of these (for example near 1400) occur at times when either θ or ϕ are at such a value as to preclude intersection of the IMF line with the bow shock. The origin of these fluxes remains unknown, although they may well be associated with local solar wind-lunar interactions. However, the bow shock events are distinguished not only by their dependence upon the IMF direction, but also by their greater intensity.

Electron spectra for the longer duration bow shock events were computed from 30-minute averages. These long averages were necessary to gain statistical significance in view of the low counting rates involved. Figure 2 shows the elctron spectrum for the period 0315-0345 on May 25, 1971, corresponding to the second large event in Figure 1. In this and other spectra the data points and standard deviations were computed with the usual statistical techniques. In order to determine densities and temperatures, a chi-squared minimization algorithm called CURFIT [Bevington, 1969] was used to fit both Maxwellians and kappa-functions [Vasyliunas, 1968] to the data points. It was found that in most cases the kappa-function, with its power-law representation of a high-energy tail resultéd in a better fit (smaller χ^2) than did the Maxwellian function. For example, for the data points of Figure 2 a Maxwellian fit resulted in the parameters $n = 2.9 \times 10^{-3}$, $T = 1.1 \times 10^6 °K$, and $\chi^2 = 0.31$ whereas a kappa-function fit resulted in $n = 3.5 \times 10^{-3}$, $T = 2.5 \times 10^6 °K$, kappa $= 3.3$ and $\chi^2 = 0.20$. The dotted line on the figure then represents the fitted kappa-function spectrum. The fitted spectra for the events studied gave densities in the range $2-4 \times 10^{-3}$ electrons/cm^3, and temperatures (thermal energies) in the range $1.7 \times 10^6 - 2.8 \times 10^6 °K$ (150-250 eV).

C. DISCUSSION

Scudder et al. [1973] report a study of solar wind electron temperatures with OGO-5 wherein they separated the data set into

two subsets based on whether or not the IMF lines through the observation point intersected the bow shock. They found a slight tendency for the electron temperature to be larger when the field lines intersected the bow shock, although the statistical reliability of the statement was greater than 50% on only one out of 5 orbits studied. (See their Table 1 and Figure 3.) They attributed these higher temperatures to a non-Maxwellian electron population with energies on the order of 100 eV. It is therefore suggested that the bow-shock-associated electron fluxes reported herein are one and the same with the electron fluxes responsible for the temperature increases reported by Scudder et al. [1973].

To emphasize this last point, in Figure 3 we have plotted a superposition of a typical solar wind electron energy spectrum as reported by Montgomery et al. [1970] with $n = 5.5$ cm^{-3} and $T_e = 1.6 \times 10^5 \, ^\circ K$ and the spectrum fitted to the data of Figure 2. The bow shock electrons appear essentially as a small high-energy tail upon the main spectrum. This high-energy tail would result in a higher temperature from a moment calculation although its true nature would be effectively masked. However, for this study the moon acted to shield the instrument from the solar wind electrons and allowed an uncontaminated measure of the properties of these bow shock electrons.

It can be easily shown that the effective temperature of the sum of two distributions $f_1(v)$ and $f_2(v)$, where $n_1 \gg n_2$ and

$T_2 > T_1$, can be approximated by $T_{eff} = T_1 + \dfrac{n_2 T_2}{n_1}$. Performing the calculation for the data shown above gives $T_{eff} = 1.62 \times 10^5$ versus $T_1 = 1.60 \times 10^5$. This small increase in effective temperature is of the same order of magnitude as that reported by Scudder et al. [1973] in their study.

Bow shock observations by Fredricks et al. [1970] indicate that the shock may be classed as turbulent, that is, ion electrostatic waves play an important role in randomizing the incoming ion stream into post-shock conditions. Yet it must be kept in mind that the shock does not act as an impenetrable wall between the pre- and post-shock plasma. Rather, there is interpenetration of ions from each region into the other, and in the shock transition itself the ion distribution becomes bimodal. This can lead to growth of wave modes which act in a self-consistent manner to convert the cool pre-shock ion distribution into the hot post-shock distribution. This intermixing of distribution functions was originally discussed by Mott-Smith [1951] in connection with classical gas shocks and a discussion applicable to collisionless plasma shocks may be found in Tidman and Krall [1971]. The upstream component of the downstream ion distribution has been observed experimentally by Montgomery et al. [1970].

By contrast the electron distribution does not become bimodal in the shock transition, and hence the conditions are not immediately available for electron electrostatic wave growth.

It is an observational fact that solar wind electrons are quite different in character from magnetosheath electrons (see, for example, Montgomery et al. [1970]), and therefore there must exist a mechanism which prevents complete mixing of the pre- and post-shock electron distributions.

Montgomery and Joyce [1969] have developed a model of a laminar electrostatic shock which provides such a mechanism. In their model the ions on both sides of the shock were at zero temperature (thus disposing of the need for an additional dissipation mechanism) while the post-shock electrons were treated as a sum of free and trapped distributions. An estimate of the potential drop across the shock can be obtained by using the measured electron spectrum (Figure 2) and a typical magnetosheath distribution [Montgomery et al., 1970] and by assuming that the Liouville Theorem applies. From the electron spectrum of Figure 2, $f_{\hat{e}}(v = 0) = 3.9 \times 10^{-30}$ cm^{-6} sec^3. This value occurs on the magnetosheath distribution at a velocity of 1.35×10^9 cm/sec corresponding to a total potential drop of 500 V. Because the measured density at $X_{SE} \cong 60$ R_E may well be lower than near the bow shock, the value of 500 V is an upper limit.

The above arguments have been necessarily ad hoc and by no means are offered as proof that such an electrostatic potential barrier actually exists. The required electron distribution separation mechanism could well be provided by other wave-related

means. However, Neugebauer [1970] reported a decrease in the solar wind ion flow energy without an increase in temperature just ahead of the bow shock, and postulated that an electrostatic potential drop with a maximum value of 200 volts was responsible. It may well be then that if a potential drop across the shock exists, then it is not confined entirely to the shock transition layer but rather is distributed also upstream and downstream of the shock.

D. SUMMARY

Low energy electrons have been observed at lunar orbit upstream of the bow shock which displayed the following characteristics:

1. The electrons were controlled by the IMF direction, appearing only when the IMF line through the observation point connected back to the bow shock.

2. Densities were in the range $2-4 \times 10^{-3}$ and temperatures (mean energies) were in the range $1.7-2.8 \times 10^{6}$ °K (150-250 eV).

The electrons were shown to be able to account for the small increases in solar wind electron temperatures on bow-shock-connected field lines observed by Scudder et al. [1973]. If it is assumed that these electrons are the high-energy tail of the magnetosheath electron distribution leaking back upstream through an electrostatic potential barrier, then a total potential drop of 500 volts is estimated. This complements an earlier observa-

tion of Neugebauer [1970] indicating a 200 volt drop in a layer immediately ahead of the bow shock. It is therefore suggested that an electrostatic potential drop which acts to prevent the majority of the downstream electron distribution from mixing with the upstream plasma deserves serious consideration in theories and models of the earth's bow shock.

REFERENCES

Anderson, K. A., Energetic electrons of terrestrial origin
behind the bow shock and upstream in the solar wind,
J. Geophys. Res., 74, 95, 1969.

Bevington, Philip R., Data Reduction and Error Analysis for
the Physical Sciences, Chapt. 11, McGraw-Hill, New York,
1969.

Burke, W. J., and D. L. Reasoner, Absence of the plasma sheet
at lunar distance during geomagnetic quiet times, Planet.
Space Sci., 20, 424, 1972.

Fredricks, R W., G M. Crook, C. F. Kennel, I. M Green, F. L
Scarf, P J. Colemen, and C. T. Russell, OGO 5 observations
of electrostatic turbulence in bow shock magnetic structures,
J. Geophys. Res., 75, 3751, 1970.

Lin, R. P, C.-I. Meng, and K. A. Anderson, 30- to 100-keV
Protons upstream from the earth's bow shock, J Geophys.
Res., 79, 489, 1974.

Montgomery, Michael D., J. R. Asbridge, and S. J. Bame, Vela 4
plasma observations near the earth's bow shock, J. Geophys.
Res., 75, 1217, 1970.

Montgomery, David, and Glenn Joyce, Shock-like solutions of the
electrostatic Vlasov equation, J. Plasma Phys., 3, Pt. 1,
1, 1969.

Mott-Smith, H., The solution of the Boltzmann equation for a

   shock wave, Phys. Rev., 82, 885,1951.

Neugebauer, Marcia, Initial deceleration of solar wind positive

   ions in the earth's bow shock, J. Geophys. Res., 75, 717,

   1970.

Scudder, J. D., D. L. Lind, and K. W. Ogilvie, Electron observa-

   tions in the solar wind and magnetosheath, J. Geophys. Res.,

   78, 6535, 1973.

Tidman, D. A., and N. A. Krall, Shock Waves in Collisionless

   Plasmas, Chap. 8, Wiley-Interscience, New York, 1971.

Vasyliunas, Vytenis M., A survey of low-energy electrons in

   the evening sector of the magnetosphere with OGO-1 and

   OGO-3, J. Geophys. Res., 73, 1968.

FIGURE CAPTIONS

Fig. 1. Low-energy electron and interplanetary magnetic field
data from May 25, 1971, showing bow-shock associated
electron events between 0210 and 0230 and again between
0305 and 0410. The dotted lines on the plot of the IMF
longitude ϕ are the limiting values for bow shock inter-
section

Fig. 2. The electron energy spectrum for the period 0315-0345
on May 25, 1971, corresponding to the second large
flux enhancement in Figure 1. The dotted line is
a kappa-function fit to the data points resulting in
the parameters $n = 3.5 \times 10^{-3}$, $T_e = 2.5 \times 10^{6} °K$, and
kappa $= 3.3$.

Fig. 3. A superposition of a typical solar wind electron spec-
trum from Montgomery et al. [1970] and the electron
spectrum of Figure 2. This shows that these bow shock
electrons result in a small increase in the effective
solar wind electron temperature.

FLUX (electrons / cm² - sr - sec - eV)

ELECTRON ENERGY (eV)